25th ABCM International Congress of Mechanical Engineering
October 20-25, 2019, Uberlândia, MG, Brazil

PRACTICAL ASPECTS BEHIND THE ROTORS FORCES TO CONTROL A QUADCOPTER

Juan Terenciani Batista[1]
Renan Sanches Geronel[2]
Douglas Domingues Bueno[3]
São Paulo State University (Unesp), School of Engineering of Ilha Solteira, Av. Brasil 56, Ilha Solteira, SP, Zip Code 15385-000, Brazil
juanterenciani2@gmail.com[1]
renansanches91@gmail.com[2]
douglas.bueno@unesp.br[3]

Abstract. *Unmanned aerial vehicles (UAVs) have been developed for several applications and purposes, mainly for the engineering field. The motion and orientation of the UAV are typically achieved using control strategies to generate combined levels of forces on each rotor to their actions on the UAV's frame. However, if a control strategy is not conveniently defined, the UAV can exhibit undesired motions, like oscillations around target trajectory. In this context, this present paper investigates and discusses this practical aspect of operating a quadcopter UAV-type vehicle. The mathematical model is obtained considering the kinematics and dynamics equations. Three different strategies of control the UAV are discussed and, using the best strategy, a second UAV configurations is evaluated too. This second one consists to comprise a coupled mass on the quadcopter attached by a linear spring. The results herein show that a design of UAV control laws must be carefully defined to establish a high efficient areal vehicle.*

Keywords: *Unmanned Aerial Vehicle, Control Strategies for UAVs, Undesired Oscillations, Coupled Mass.*

1. INTRODUCTION

The research in the area of quadcopters, also refered to as Unmanned Aerial Vehicles (UAVs), is increasing continually because of their interesting applications. A quadcopter has a wide range of applications in several fields, such as military operations, aerial photography, rescue operations, transportations Verbeke and Debruyne (2016).

The quadcopter for agricultural surveillance survey crops and leaves reducing human efforts. An infrared camera is used to analyze the color image displaying the difference between infected or diseased cop and mature cop. Evaporation rate, water deficits, disease are some of the effects being studied by Patel *et al.* (2013).Police officers all over the word, such as, United States, UK, use quadcopters to monitor large crowds, prevent or detect crimes besides monitor huge events Ostojić *et al.* (2015).

Autonomous quadcopter are evaluated using an interfaced android device as its core. Google map is used to set the correct trajectory for delivering the product. Fuel and labor cost reduction, transportation management create a competitive advantage in market place Haque *et al.* (2014). A micro aerial vehicle platform is used to perceive obstacles and avoid collisions. Ultrasonic sensors are used to increase detection resolution and sensor data reliability and all signals from sensors are processed by Arduino board Salaskar *et al.* (2014).

Tamami *et al.* (2014) uses a combination of PD (proportional-derivative) controller and PIAFC (proportional integral active force control) to present a stabilize quadcopter, where the first one stabilize properly and PIAFC is used to reject uncertainty disturbance (e.g. wind). It is also made a comparison among three different controllers (PD,PD-AFC,PD-PIAFC) and it is shown the last combination exhibits better performance and gives the smaller error. The best result of the controller is presented by PD-PIAFC compared with the others, showing the lowest RMS value of control signal for constant and even fluctuated disturbance.

Ahmad *et al.* (2018) compares two classical controllers (PD and PID) to propose a control strategy for attitude (roll, pitch, and yaw) and altitude (height). To do this, two control loops are used. The first control loop is responsible for attitude (Euler angles are required). The second control loop is for controlling the altitude, where the height is necessary for that. It can be concluded PD gives better results for attitude control, whereas PID gives better for altitude. Mituleţu *et al.* (2018) describes an adaptive tuning control of a quadcopter using PID technique. Different outputs and proper PID gain sets are tested reaching the steady state level to almost three times faster than usual controller.

The quadcopter is modeled with four rotors in a cross configuration. When this system is performing a motion, it exhibits an angular speed that creates a thrust force, consequently, a specific torque in each propeller. In particular, this work proposes to study the mathematical modeling of the coupled system and discuss the contributions of a combination of torques to describe and analyze the desired path. Furthermore, a coupled mass is added to the quadcopter configuration,

showing the effect it may be caused using different stiffness.

2. METHODOLOGY

The mathematical modeling of a quadcopter proposed by Kim *et al.* (2009) can be represented below. The dynamic equation of motion 1 derived in earth-fixed coordinate frame is expressed:

$$\mathbf{M}_\eta \ddot{\boldsymbol{\eta}} + \mathbf{C}_\eta \dot{\boldsymbol{\eta}} + \boldsymbol{g}_\eta = \boldsymbol{\tau}_\eta \tag{1}$$

where, the quadcopter generalized position coordinates could be expressed by:

$$\boldsymbol{\eta} = \{x, y, z, \phi, \theta, \psi\}^T \tag{2}$$

Then, the system matrices are defined as below:

$$\mathbf{M}_\eta = \mathbf{J}^{-T}\mathbf{M}\mathbf{J}^{-1} \tag{3}$$

$$\mathbf{C}_\eta = \frac{1}{2}\dot{\mathbf{M}}_\eta \tag{4}$$

$$\boldsymbol{g}_\eta = \{0, 0, g, 0, 0, 0\}^T \tag{5}$$

$$\boldsymbol{\tau}_\eta = \mathbf{J}^{-T}\boldsymbol{\tau} \tag{6}$$

The matrix $\mathbf{M}$ is expressed by:

$$\mathbf{M} = \begin{bmatrix} m & 0 & 0 & 0 & 0 & 0 \\ 0 & m & 0 & 0 & 0 & 0 \\ 0 & 0 & m & 0 & 0 & 0 \\ 0 & 0 & 0 & I_{xx} & 0 & 0 \\ 0 & 0 & 0 & 0 & I_{yy} & 0 \\ 0 & 0 & 0 & 0 & 0 & I_{zz} \end{bmatrix} \tag{7}$$

In this work, the modeling of a quadcopter includes the structure along with dynamic of engines, besides aerodynamic efects and gyroscopic effect. Figure 1 shows coordinate systems of UAV.

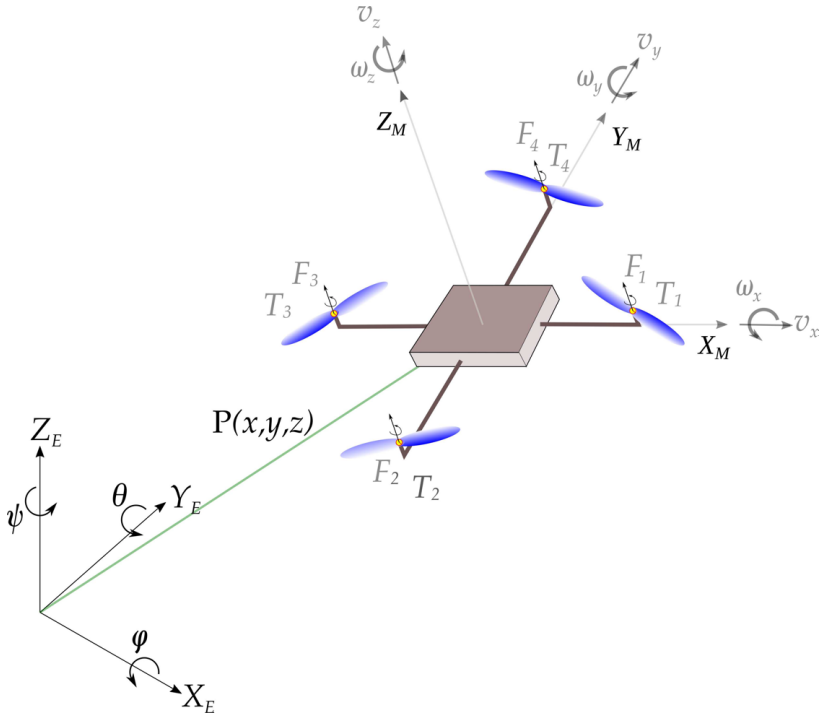

Figure 1. Coordinate system.

In this work is used the strategy of control that separate dynamic of rigid body and the structure. It is assumed by reference two cordinate systems, i.e., intertial reference frame $R_i(E_1, E_2, E_3)$ and body-fixed reference frame $R_a(e_1, e_2, e_3)$. The transformation matrix between two frames is denoted by J as given in Eq. 8.

$$\mathbf{J} = \begin{bmatrix} c\theta c\phi & s\psi s\theta c\phi - c\psi s\phi & c\psi s\theta c\phi + s\psi s\phi & 0 & 0 & 0 \\ c\theta s\phi & s\psi s\theta s\phi + c\psi c\phi & c\psi s\theta s\phi + s\psi c\phi & 0 & 0 & 0 \\ -s\theta & s\psi c\theta & c\psi c\theta & 0 & 0 & 0 \\ 0 & 0 & 0 & 1 & s\phi t\theta & c\phi t\theta \\ 0 & 0 & 0 & 0 & c\phi & -s\phi \\ 0 & 0 & 0 & 0 & s\phi/c\theta & c\phi/c\theta \end{bmatrix} \tag{8}$$

where $c(\cdot)$, $s(\cdot)$ and $t(\cdot)$ are, respectively, cosine, sine and tangent.

Dynamic model of the quadcopter is obtained by analyzing various forces and torques acting on it. Some assumptions are made as follows: the body of quadcopter is rigid, four DC motors are indepedent, each motor of the quadcopter rotates a propeller, and two opposite propellers rotate in same direction for balacing the quadcopter.

The differences in four angular speeds result in motion of UAV. Roll, pitch and yaw angles are denoted by θ, ϕ and ψ, respectively. The angular speeds of left, back, right and front propellers are denoted by ω_1, ω_2, ω_3, and ω_4. The pitch motion is obtained through ω_2 minus ω_4. Similarly, ω_1 minus ω_3 cause a roll motion. Finally, the yaw motion ψ of the quadcopter is caused when algebraic sum of moments produced by four propellers is not zero, i.e., there is difference in angular speeds between two opposite pairs of propellers. Figure 2 illustrates the combination of the quad rotor speeds and their resulting torque τ are given by

$$\boldsymbol{\tau} = \left\{ \begin{array}{cccccc} 0 & 0 & (F_1 + F_2 + F_3 + F_4) & (-F_2 + F_4)l & (-F_1 + F_3)l & (-F_1 + F_2 - F_3 + F_4)\lambda \end{array} \right\}^T \tag{9}$$

where l is the distance between the motor and the center of mass; F_i are the thrust forces of the four propellers (the subscript i denotes the number of propeller i=1,2,3 or 4), λ is the relation between torque and generated force.

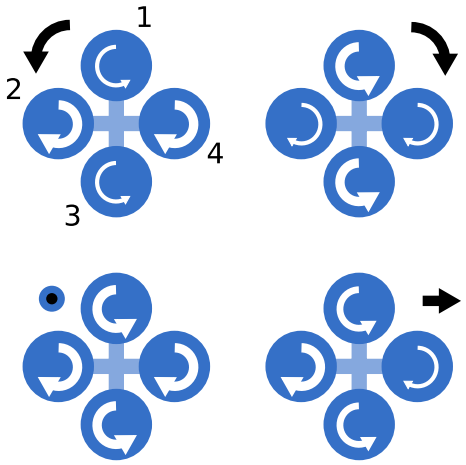

Figure 2. UAV motion principle. Reproduced from Kim *et al.* (2009).

2.1 Quadcopter Dynamics including a Coupled Mass

The UAV dynamics is also evaluated in this study considering a coupled mass m_c. It is considered attached to the quadcopter frame struct, as illustrated in Fig. 3. Each equation previously discussed are similar to this case. However, it is included additional terms to couple the preliminary system of equations to this new degree of freedom (see that the coupled mass is fixed by using a linear spring with stiffness k_c).

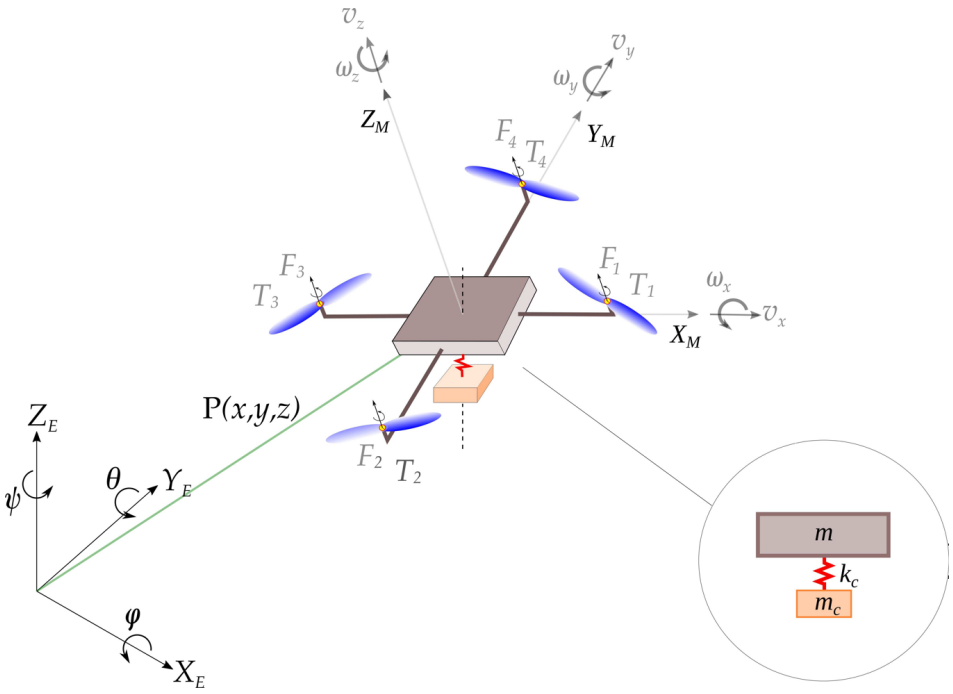

Figure 3. Quadcopter reference system including the coupled mass.

For this condition, the new general equation of motion is given by Eq. 10. In Considering the inertial reference frame, the stiffness matrix $\boldsymbol{K}_{\eta_c}$ is expressed by Eq. 11, where $\mathbf{0}_{(5\times7)}$ is a matrix of zeros, with dimensions of (5,7) e k_c is the stiffness for the coupling system.

$$\mathbf{M}_{\eta_c}(\boldsymbol{\eta}_c)\ddot{\boldsymbol{\eta}}_c + \mathbf{C}_{\eta_c}(\boldsymbol{\nu},\boldsymbol{\eta}_c)\dot{\boldsymbol{\eta}}_c + \mathbf{g}_{\eta_c}(\boldsymbol{\eta}_c) + \boldsymbol{K}_{\eta_c}(\boldsymbol{\eta}_c)\boldsymbol{\eta}_c = \boldsymbol{\tau}_{\eta_c}(\boldsymbol{\eta}_c) \tag{10}$$

$$\mathbf{K}_{\eta_c} = \begin{bmatrix} 0 & 0 & k_c & & & & -k_c \\ & & & \mathbf{0}_{(5\times7)} & & & \\ 0 & 0 & -k_c & & & & k_c \end{bmatrix} \tag{11}$$

Also, the new mass matrix is described by $\mathbf{M}_{\eta_c}$ such that:

$$\mathbf{M}_{\eta_c} = \begin{bmatrix} \mathbf{M} & \mathbf{0}_{(6\times1)} \\ \mathbf{0}_{(1\times6)} & m_c \end{bmatrix} \tag{12}$$

where $\mathbf{M}$ is the mass matrix, $\mathbf{0}_{(6\times1)}$ and $\mathbf{0}_{(1\times6)}$ matrices of zeros dimensioning (6,1) and (1,6), respectively. Therefore, m_c is the mass added, described by the mass-spring as following. Similarly to the mass matrix, the Jacobian matrix is added a new degree of freedom, which in this case, the studied case only translates in the vertical direction z. The relation between the inertial and body-fixed reference frame can be expressed by:

$$\begin{Bmatrix} \dot{\boldsymbol{\eta}} \\ \dot{\mathbf{z}}_c \end{Bmatrix} = \mathbf{J}(\boldsymbol{\eta}_c) \begin{Bmatrix} \boldsymbol{\nu} \\ \dot{\mathbf{z}}_c \end{Bmatrix} \tag{13}$$

where the original Jacobian matrix to rotations is kept. Evaluating the mass-spring adding, there is a velocity $\dot{\mathbf{z}}_c$ described in the body-fixed reference frame (quadcopter's body), wherein any time, has been parallel to the inertial reference frame. Thereby, a new degree of pure translation is observed to this coordinate, which the unitary value can be adopted to its transformation.

$$\mathbf{J}(\boldsymbol{\eta}_c) = \begin{bmatrix} \mathbf{J}(\boldsymbol{\eta}) & \mathbf{0}_{(6\times1)} \\ \mathbf{0}_{(1\times6)} & 1 \end{bmatrix} \tag{14}$$

where, in this case, $\boldsymbol{\eta}_c$ is given by:

$$\boldsymbol{\eta}_c = \begin{Bmatrix} x & y & z & \phi & \theta & \psi & z_c \end{Bmatrix}^T \tag{15}$$

3. RESULTS AND DISCUSSIONS

Using the mathematical modeling previously introduced, it is possible to evaluate different strategies to control the UAV trajectory during the flight. The main idea is to understand basic dynamic characteristics resulting from the control rule established. Numerical simulations are carried out using the parameters shown in Table 1 and employing the 4-th order Runge-Kutta algorithm.

Table 1. Parameters of the quadcopter.

$Parameters[Units]$	$m\ [kg]$	$l\ [m]$	$\lambda\ [ms^2]$	$I_{xx}\ [kgm^2]$	$I_{yy}\ [kgm^2]$	$I_{zz}\ [kgm^2]$	$g\ [m/s^2]$
$Values$	2.2	0.1725	1	0.0167	0.0167	0.0231	9.81

For this study, three different strategies are defined to altitude control. In this sense, the control strategy is the input and the altitude (Z) is the UAV output. The strategies are chosen arbitrarily to illustrated different operational conditions. Each strategy A, B and C is described by the lift force F_Z^N, $N = A, B$ or C, and they are defined as follows:

$$F_Z^A = \begin{cases} 2mg & \text{, if} \quad Z \leqslant h \quad \text{and} \quad \dot{Z} < 0 \\ 1.25mg & \text{, if} \quad Z \leqslant h \quad \text{and} \quad \dot{Z} \geqslant 0 \\ 0.5mg & \text{, if} \quad Z > h \end{cases} \tag{16}$$

$$F_Z^B = \begin{cases} 2mg & \text{, if} \quad Z \leqslant (h-d) \quad \text{and} \quad \dot{Z} < 0 \\ 1.25mg & \text{, if} \quad Z \leqslant (h-d) \quad \text{and} \quad \dot{Z} \geqslant 0 \\ 1mg & \text{, if} \quad Z > (h-d) \quad \text{and} \quad Z < (h+d) \\ 0.5mg & \text{, if} \quad Z > (h+d) \end{cases} \tag{17}$$

$$F_Z^C = \begin{cases} 2mg & \text{, if} \quad Z \leqslant (h-d) \quad \text{and} \quad \dot{Z} < 0 \\ 1.25mg & \text{, if} \quad Z \leqslant (h-d) \quad \text{and} \quad \dot{Z} \geqslant 0 \quad \text{and} \quad \dot{Z} < \sqrt{g(h-d-Z)} \\ 1mg & \text{, if} \quad Z > (h-d) \quad \text{and} \quad Z < (h+d) \\ 0.5mg & \text{, if} \quad Z > (h+d) \quad \text{or} \quad \dot{Z} \geqslant \sqrt{g(h-d-Z)} \end{cases} \tag{18}$$

where Z is the UAV altitude, $\dot{Z}$ is its altitude variation over time, h is the desired altitude, d is a tolerance for this altitude and F_Z^N is the lift signal that control N requests UAV to deliver. Considering no delay between the output of control N and the response of the UAV system, it is assumed that the lift requested by control N is the same as the lift signal of the UAV. Also note that:

$$\ddot{Z}m = F_Z - mg \tag{19}$$

where $\ddot{Z}$ is the acceleration of the UAV at its altitude over time. Based on this equation is easy to note that no altitude variation is observed if F_Z is equal to mg.

The study of the UAV altitude for each control strategy considers a target defined as $h = 2$ meters. The idea behind this study is to evaluate eventual transient before the quadcopter stabilize itself at this target altitude. It is assumed as acceptable an altitude deviation d equal to 0.05 meters, starting the motion from initial conditions equals to $Z_0 = 0$ and $\dot{Z}_0 = 0$. Figures 4 to 6 show the input (the lift force, i.e., the upper red line) and each corresponding UAV altitude (the bottom blue line).

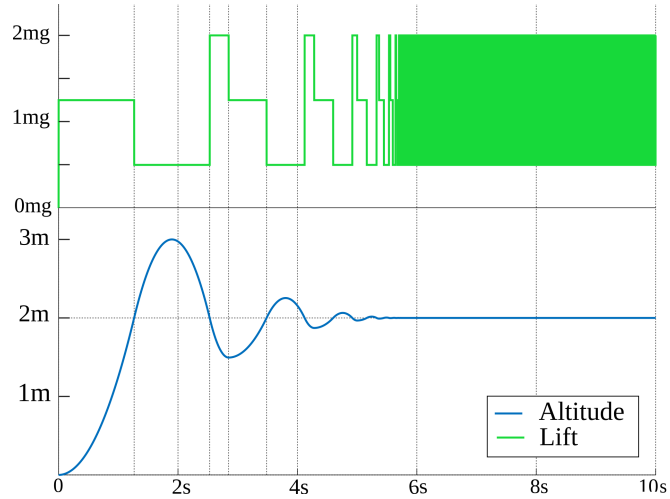

Figure 4. Lift force and UAV altitude over time: control strategy A.

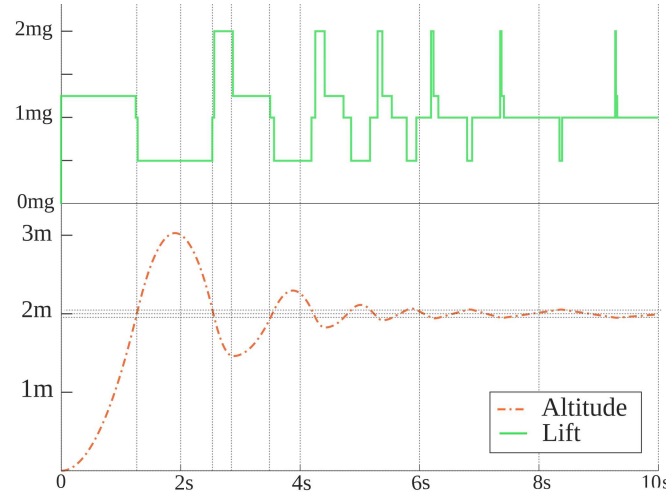

Figure 5. Lift force and UAV altitude over time: control strategy B.

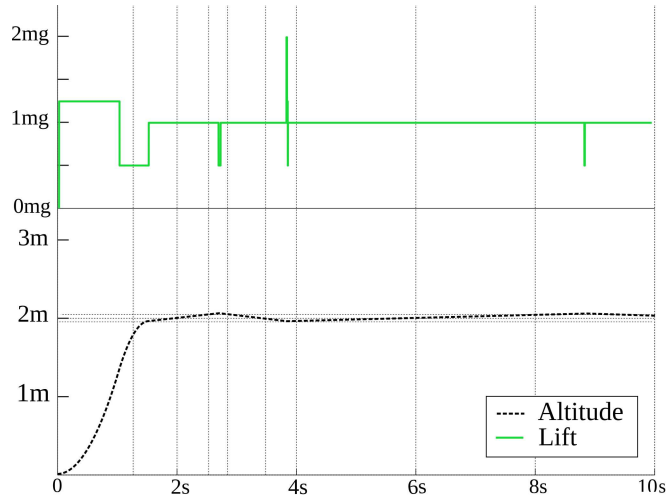

Figure 6. Lift force and UAV altitude over time: control strategy C.

The level of required force to evaluate each control strategy, the RMS (root mean square) value is computed for each lift force (Eq. 20). It is an important parameter to evaluate the operational life of the energy source, as the typical batteries used in this type of vehicles. Using this approach, the following values were found respectively to the control strategies A, B and C: 24.863 N, 23.502 N and 22.223 N.

$$F_{Z,RMS} = \sqrt{\frac{1}{N}\sum_{i=1}^{N}(F_{Z,i})^2} \tag{20}$$

Based on the results, control strategy A exhibits a better and faster convergence than control B, but both of them present important overshoot, implying to the quadcopter achieves an incorrect altitude during flight. However, control strategy C exhibits the best performance, also requiring lower ratio of lift over time. A comparison among these strategies is shown in Fig. 7, where the UAV altitude can be observed for each case. In addition, the lift spectral amplitude are shown in Fig. 8. It is possible to see that control strategy A applies a high level of power on the quadcopter. These results also show that strategies B and C present similar levels of power, although in the this last case the system exhibits a quasi non oscillatory motion until the UAV flies to achieve the target altitude.

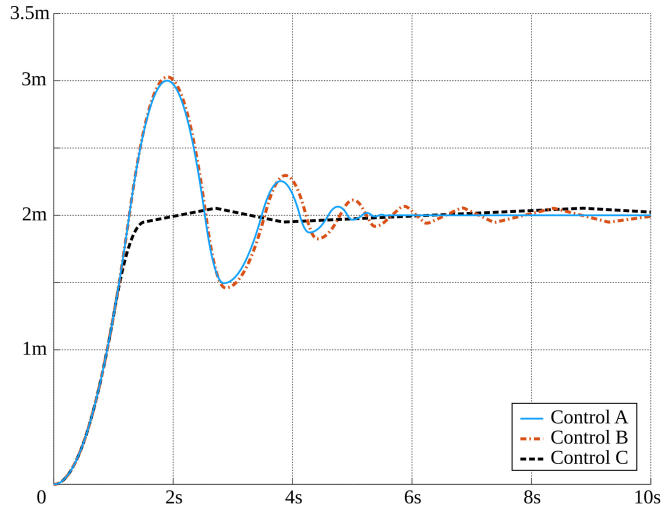

Figure 7. Comparison of the UAV altitude for each control strategy investigated.

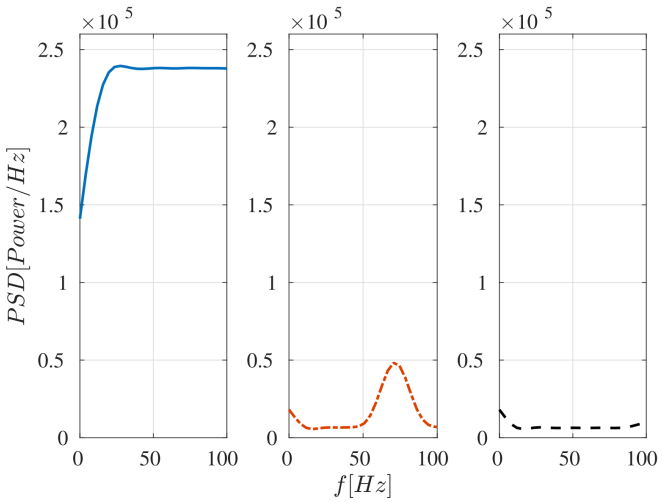

Figure 8. Lift power spectral density: control A (blue line, left hand side), control B (dotted orange line, center), and control C (black dashed line, right hand side).

Coupled Mass on the UAV

The dynamics of the UAV is also investigated using the control strategy C for a second quadcopter configuration. In this second one, a coupled mass is considered attached to the UAV's frame struct. It is used a linear spring with two different stiffness $k_c i$, $i = 0, 1$, as shown in Tab. 2. The first shown in Fig. 9 demonstrate a low oscillatory behavior of the coupled mass around the UAV position, although the best control strategy has been employed. In other and, after considering a higher level of stiffness, the couple mass presents the same shape of motion in comparison with the quadcopter, as shown in Fig. 10. Based on this results, it is possible to understand that a control strategy for an UAV must consider the on board subsystem dynamics to design an high efficient areal vehicle.

Table 2. Parameters of the quadcopter.

Parameters	$m\ [kg]$	$m_c\ [kg]$	$k_{c0}\ [N/m]$	$k_{c1}\ [N/m]$
Values	2.2	0.22	50	500

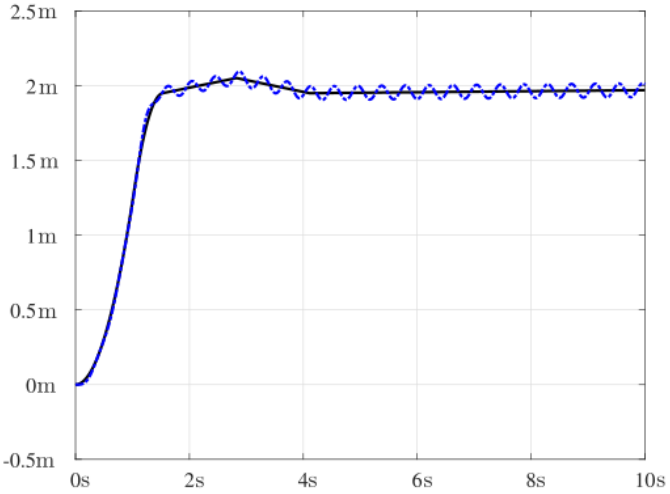

Figure 9. Quadcopter altitude (black line) and coupled mass motion (blue dashed line) for $k_c = 50N/m$.

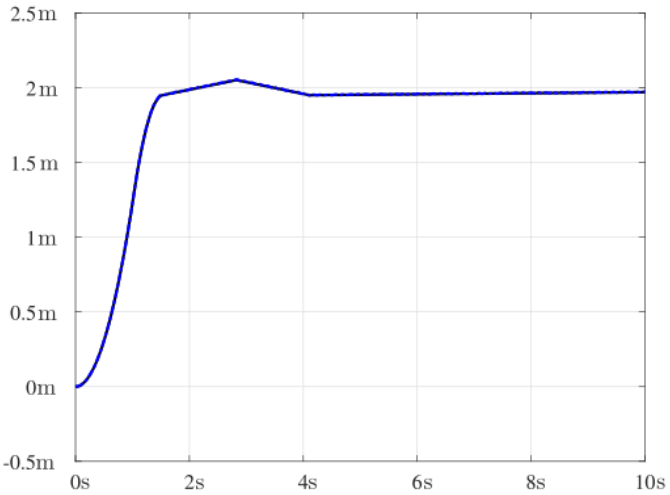

Figure 10. Quadcopter altitude (black line) and coupled mass motion (blue dashed line) for $k_c = 500N/m$.

4. FINAL REMARKS

Based on the quadcopter mathematical model and using a numerical method to integrate the equation of motion, this work compares three altitude control strategies allowing to compare the time to achieve a desired altitude during the flight. It is also evaluated the energy efficiency, in terms of RMS levels of the required force to control the vehicle. Strategy of Control C excelled in both criteria once, it uses a method that considers the difference of mechanical energy between the desired and real positions. In other hand, Control A caused the lift force to vary at a very high frequency, as it did not use a tolerance of the desired position. Besides that, power spectral density is calculated to evaluate the quantity of power for each frequency component. Finally, it's also shown three situations using different values of stiffness and its performance, when a mass is coupled. These results shown that special attention must be given to design controllers for quadcopter UAVs, mainly when they transport addition mass attached on their frame struct.

5. ACKNOWLEDGEMENTS

The authors would like to express their appreciation to São Paulo State University (Unesp) - Feis - Ilha Solteira, in particular the Departments of Mechanical Engineering and Mathematics; and to National Council for Scientific and Technological Development (CNPq) *Edital* Universal 429963/2016-5

6. REFERENCES

Ahmad, F., Kumar, P. and Patil, P.P., 2018. "Modeling and simulation of a quadcopter with altitude and attitude control." *Nonlinear Studies*, Vol. 25, No. 2.

Haque, M.R., Muhammad, M., Swarnaker, D. and Arifuzzaman, M., 2014. "Autonomous quadcopter for product home delivery". In *2014 International Conference on Electrical Engineering and Information & Communication Technology*. IEEE, pp. 1–5.

Kim, J., Kang, M.S. and Park, S., 2009. "Accurate modeling and robust hovering control for a quad-rotor vtol aircraft". In *Selected papers from the 2nd International Symposium on UAVs, Reno, Nevada, USA June 8–10, 2009*. Springer, pp. 9–26.

Mituleţu, I.C., Spunei, E., Markovican, E. and Popescu, I., 2018. "Quadcopter stability increased by pid adaptive tuning." *Analele Universitatii'Eftimie Murgu'*, Vol. 25, No. 2.

Ostojić, G., Stankovski, S., Tejić, B., Đukić, N. and Tegeltija, S., 2015. "Design, control and application of quadcopter". *Int. J. Ind. Eng. Manag*, Vol. 6, pp. 43–48.

Patel, P.N., Patel, M.A., Faldu, R.M. and Dave, Y.R., 2013. "Quadcopter for agricultural surveillance". *Advance in Electronic and Electric Engineering*, Vol. 3, No. 4, pp. 427–432.

Salaskar, P., Paranjpe, S., Reddy, J. and Shah, A., 2014. "Quadcopter–obstacle detection and collision avoidance". *Int. J. Eng. Trends Technol*, Vol. 17, No. 2, pp. 84–87.

Tamami, N., Pitowarno, E. and Astawa, I.G.P., 2014. "A combination of pd controller and piafc for stabilization of ŞxŤ configuration quadcopter". *EMITTER International Journal of Engineering Technology*, Vol. 2, No. 1, pp. 1–16.

Verbeke, J. and Debruyne, S., 2016. "Vibration analysis of a uav multirotor frame". In *International Conference on Noise and Vibration Engineering*.